The Fundamental Motor of the Human Neutrophil Is Not Random: Evidence for Local Non-Markov Movement in Neutrophils

R. S. Hartman, K. Lau, W. Chou, and T. D. Coates
Division of Hematology-Oncology, Childrens Hospital, University of Southern California School of Medicine, Los Angeles, California 90027 USA

ABSTRACT The search for a fundamental mechano-chemical process that results in net cell motion has led investigators to fit neutrophil tracking data to well described physical models in hopes of understanding the functional form of the driving force. The Ornstein-Uhlenbeck (OU) equation for mean square displacement describes a locally persistent and globally random process and is often used as a starting point for analysis of neutrophil displacements. Based upon the apparently close fit of neutrophil tracking data to this equation and the nature of its derivation, biologists have inferred that the motor of the neutrophil is best represented as a random process. However, 24 of 37 neutrophil paths that we investigated preferentially display programmatic rather than Markov short term correlations between displacements or turn angles. These correlations reflect a bimodal rather than a uniform distribution of subpath correlations in the two variables, and are strongly sampling rate-dependent. Significant periodic components of neutrophil shape change are also detected at the same time scale using either Fourier or elliptical Fourier transform-based descriptors of the neutrophil perimeter. Oscillations in neutrophil velocity have the same period. Taken together, these data suggest a nonstochastic, and perhaps periodic, component to the process driving neutrophil movement.

INTRODUCTION

Neutrophils (polymorphonuclear leukocytes, PMN) circulate passively in the blood stream until activated and recruited to a site of infection. Molecular species produced by invading microorganisms promote the activation event and provide a chemoattractant gradient that the neutrophil will follow (Baggiolini and Kernen, 1992; Cassimeris and Zigmond, 1990). Attempts to understand the mechanism of crawling by which the neutrophil transits the endothelium and intervening tissue to the phagocytic site have led to measurements of neutrophil shape change and movement in various one, two, and three-dimensional in vitro systems (Senda et al., 1975; MacFarlane et al., 1987; Needham and Hochmuth, 1992; Coates et al., 1992). The most direct expression of the neutrophil motor is local cell shape change. It is at the level of shape change that the fundamental impetus to cell movement is first manifest. Motion at distances greater than one cell diameter must then result from iterations of this fundamental motion. There are several measures potentially useful in identifying expressions of the fundamental mechanism.

The basic measurement parameter of choice in several previous studies has been the mean square point-to-point displacement $\langle h^2 \rangle$ of the moving cell. This parameter simply measures the net distance traveled by a cell during a specified length of time, usually recorded as a specified number of video frames. A function may be constructed, for example, by averaging over all distances travelled by the cell in each range of 1 frame to 25 frames. Actual travel times represented will depend on the frame-rate. Experimental values of $\langle h^2 \rangle$ for any desired number of steps may be easily extracted from cell centroid tracking data. Fundamental theory carrying only a few unknown parameters is available that relates macroscopic $\langle h^2 \rangle$ values to assumed underlying physical processes (Uhlenbeck and Ornstein, 1930; Doob, 1942). However, fitting experimental displacement data to these theoretical expressions should not be done without considering inherent correlations between $\langle h^2 \rangle$ values (Dickinson and Tranquillo, 1993). This technical point alone casts doubt on much previous quantitative analysis of mean squared displacements.

An alternate method of analysis is determination of the autocorrelation function for movement variables. This may be considered a more basic attack than analysis of $\langle h^2 \rangle$ as the latter may be derived from the velocity correlation function (Dunn and Brown, 1987; Nafe et al., 1991). If a random mechanism determines the variable in question, then either the autocorrelation function or its envelope will display monotonic decay (Bowerman and O'Connell, 1987). One may hope to detect regularities impressed on a variable in a continuous or non-continuous way by a non-random motor through deviations from monotonic decay. Both classical and vector autocorrelation treatments of experimental time series may be employed to generate autocorrelation functions. Necessary non-trivial corrections (Dunn and Brown, 1987) to the simply calculated correlation are required to allow straightforward interpretation of the data, though estimates of significance and issues of stationarity remain intertwined (Harvey, 1993).

A third approach is direct observation of (or exhaustive failure to observe) consistent patterns of geometric variation in cell shape during movement. Use of differential area, perimeter or radius maps (Dunn and Brown, 1987; Nafe et al., 1991) coupled with a time or frequency (Fourier) analysis of

Received for publication 21 October 1994 and in final form 31 March 1994.
Address reprint requests to Thomas D. Coates, M.D., Division of Hematology-Oncology, Childrens Hospital Los Angeles, 4650 Sunset Blvd, Los Angeles, CA 90027. E-mail: tom@hemonc.usc.edu.

0006-3495/94/12/2535/11 $2.00

the difference functions represents one line of attack. Alternately, one may perform the geometric analysis in frequency space by constructing descriptors from spatial frequency variables (Partin et al., 1989). These variables can then be subjected to Fourier temporal frequency analysis to uncover periodic behavior.

An observer of neutrophil crawling sees periods of persistent net movement interspersed with periods of seemingly random searches. The neutrophil paths shown in Fig. 1 demonstrate these competing tendencies. Although worm-like-chain (WLC) models originated in the physics of Brownian motion for a dilute gas (Uhlenbeck and Ornstein, 1930), extension of the theory is natural to other systems exhibiting both local persistence of behavior and global indirection. The practical usefulness of the WLC expression for describing cell movement is its robustness. In Eq. 1 we present a form of the WLC relation derived by Doob (1942).

$$\langle h^2 \rangle = 4 * \frac{\sigma^2}{\beta^2} (\beta * t - 1 + \exp(-\beta * t)) \qquad (1)$$

Here, $\langle h^2 \rangle$ is the mean square displacement of the cell during any travel time t. For long times $\langle h^2 \rangle$ is proportional to t. Pure random motion defined by the diffusion equation (Einstein, 1905) obeys this law. For short times, $\langle h^2 \rangle$ is proportional to t^2, as can be seen by expanding the exponential. This is a property of uniform motion. Times, long and short, are understood with respect to the damping parameter (β). These two cases may form the bounds of actually observed cell movement though self-avoidance, or attraction by other cells would tend to expand or collapse displacements expected from the literal form of Eq. 1.

Parameter σ is the rms cell speed, whereas β quantitatively measures the range of a Markov velocity process of any dimension through the correlation function defined by Eq. 2.

$$\rho_{31} = \exp(-\beta * (t_3 - t_2)) * \exp(-\beta * (t_2 - t_1)) \qquad (2)$$

Exponentially decaying memory of past events (e.g., cell velocity) defines a Markov process (Kleinrock, 1975). Equation 2 illustrates both this decay between times t_1 and t_3 and the decomposition of the process into several subprocesses or steps. An exact expression for one-dimensional displacement autocorrelations has been presented by Doob (1942). The form of the WLC equation for $\langle h^2 \rangle$ given in Eq. 1 is derived from Eq. 2. Under the assumptions that the stochastic force term $B(t)$ in the Langevin equation (Eq. 3)

$$dv/dt = -\beta * v + \sqrt{\alpha * B(t)} \qquad (3)$$

has zero mean and is velocity-independent, Eq. 1 may be re-derived with the constant coefficient rewritten as a ratio of stochastic variance to velocity dependent damping (Uhlenbeck and Ornstein, 1930; Doob, 1942).

$$\langle h^2 \rangle = 2 * (\alpha/\beta^3) * (\beta * t - 1 + \exp - \beta * t) \qquad (4)$$

A physical model of movement is then evident. Stokes et al. (1991), applying this analysis to cell movement, are particularly clear in assigning both random impetus and deterministic damping functions to internal cell processes. According to the standard model as expressed by Stokes, the neutrophil "motor" would produce only a random velocity process; persistent behavior is determined only by resistance to change.

The validity of Eq. 1 does not, however, depend on a velocity process that follows Eq. 3. The WLC relation (Eq. 1) may be derived assuming elastic bending of an otherwise linear object (Landau and Lifshitz, 1958); the correlation between bending angles damps exponentially. It is also a small exercise to generate by recursion data closely satisfying the WLC relation from the deterministic "logistics" equation. The chemosensory movement model of Tranquillo and Lauffenburger practically requires internal correlation as a determinant of turn angles and yet produces simulation data (Tranquillo and Lauffenburger, 1987) that closely follow Eq.1. In addition, neutrophil-neutrophil interaction in chemotactic assays appears to produce markedly higher crawling speeds at the front edge of the expanding cell mass (Quitt et al., 1990) than near the center. Neutrophils stimulated with a chemoattractant such as FMLP are reported to move somewhat faster than unstimulated cells and may also obey a WLC relation for total path displacement (Allen and Wilkinson, 1978; Gruler and Bültmann, 1984). Neutrophils will move up a chemoattractant gradient in a "snake-like" fashion (Nossal and Zigmond, 1976; MacFarlane et al., 1987). This may imply amplification of some internal cell program, not specific to the stimulated cell, that produces such correlated motion mediated by surface receptor sensing of spatial variations in external stimulant concentration (Alt, 1980; Tranquillo and Lauffenburger, 1987).

Several previous workers (Odell, 1984; Oster, 1984) have presented elegant mathematical treatments of neutrophil motility in an attempt to understand how these cells move. Because the displacements in many PMN tracks are in remarkable agreement with Eq. 1, the fundamental processes underpinning such equations have been assumed to drive PMN motion. Equation (1) may be derived with the assumption of a random driving force. Because of this, the process that drives PMN movement has been considered to be random and correlations between movement variables to be Markov (Stokes et al., 1991; Dunn and Brown, 1987; Gruler and Bültmann, 1984). In this report, we present evidence that local movement of neutrophils, as measured by displacement magnitudes and the cosine of the turn angle, may display a correlated, non-Markov component. This observation suggests deterministic cellular motion programs, although the same data also follow the WLC equation, which suggests random driving forces. Such conflicts make the simple point that attacks on problems of cell movement need a heuristic bent and raise the fascinating possibility that the driving motor of the neutrophil may express programmed periodic components.

MATERIALS AND METHODS

Cell preparation and tracking

Human neutrophils were prepared under endotoxin-free conditions from heparinized venous blood drawn by standard methods (Coates et al., 1987;

Boyum, 1984; Howard et al., 1990). The PMN were suspended in HEPES-buffered saline, pH 7.4 (10 mM HEPES, 130 mM NaCl, 5 mM KCl, 5 mM glucose, 1 mM $CaCl_2$, and 1 mM $MgCl_2$. All experiments were performed under endotoxin-free conditions (Howard et al., 1990)).

Fluorescent imaging of moving neutrophils was performed at 37°C using a Nikon Diaphot inverted microscope equipped with a 40× oil immersion objective. A video camera and image intensifier are attached to the microscope. Images are recorded on a Panasonic OMDR through a frame grabber (Imaging Technologies, Woburn, MA). Neutrophils are isolated and loaded with the calcium-sensitive fluorescent dye FURA-2 according to standard procedures (Jaconi et al., 1988) and are observed moving on albumin-coated coverslips in a Stotler chamber (Dvorak and Stotler, 1971). Images were acquired every 4 s per image pair (at 360 and 380 nm) during ratio calcium measurements.

Only cells that were actively moving without prolonged periods of quiescent or pure searching (secondary pseudopod extension) behavior were selected for analysis. We normally observe about two-thirds of the cells in a 40× field spontaneously exit the "attachment" state within several minutes. This occurs even though there has been no external addition of chemoattractant. Movement initiates with extension of the primary pseudopod and continues with the cell exhibiting overall polarization coupled to cycles of extension and contraction (Jaconi et al., 1991; Parkhurst and Saltzman, 1992). Paths involving neutrophil-neutrophil contact were excluded from study, as were paths shorter than 64 steps. It is not possible, however, to discount cell-cell interactions at distances of 1 or 2 cell diameters (Gail and Boone, 1970). Path lengths vary from 70 to 200 steps (frames). End-to-end displacements range from 17 to 75 microns.

Cell position was defined as the unweighted center of the set of coordinates defining the cell perimeter of the 380 nm fluorescent image. A standard edge detection algorithm was employed and, under our experimental conditions, produced coordinate values insensitive to required filtering and intensity threshold bounds for cell recognition. Details of analysis have been presented elsewhere (Hartman et al., 1993b). Using a 40× objective, the average diameter of the image of a single PMN is approximately 60 pixels. Thus, changes in the shape of the cell result in detectable changes in the position of the center.

Cell displacements were calculated by differencing successive cell position coordinates. Turn angles, expressed as the cosine of the angle between successive displacements, were calculated from the dot product between successive displacements. Mean square cell displacements on one path are calculated for step lengths between 1 and 25 (times between 4 and 100 s) by averaging all such values between the 1st and N-25th point on the path. Thus, an equal number of values are acquired at each n-step separation value, avoiding bias of our calculations by short displacement intervals. A similar set of calculations was performed for step lengths between 1 and 60. To demonstrate that the experimental data we obtained are very similar to those reported by previous workers, we calculated the WLC regression line with Origin 4.0 (Microcal Inc., Northampton, MA) using averaged values of $\langle h^2 \rangle$ at each time point. Fit parameters were constrained to physically meaningful values, and the found values were checked for consistency by recalculation of experimental displacements using Eq. 1.

Correlation functions

Autocorrelation of vector displacements was performed following Dunn and Brown (1987).

$$R_k = \frac{1}{(N-k)} \sum_{i=1}^{N-k} (\mathbf{d}_i * \mathbf{d}_{i+k}) \tag{5}$$

where the dot product operates between successively lagged displacements.

The experimental autocorrelation functions for turn angle and magnitude of displacements were calculated from the usual definition (Eq. 4) (Rabiner and Gold, 1975).

$$R(\tau) = \frac{1}{N} \sum_{t=1}^{N} d(t)d(t+\tau) \tag{6}$$

In this case $d(t)$ is the element of the measured displacement or turn angle ($\cos\theta$) time series found at time t for a series of N elements. Values of the autocorrelation and partial autocorrelation function averaged for subsets of the total path length were also calculated.

Measurement error corrections to the step-lag one value of both autocorrelation functions may be demonstrated and can have a significant quantitative effect on partial autocorrelation calculations. For the displacement vector autocorrelation under the assumption of uncorrelated errors, it is not difficult to derive a result already stated by Dunn and Brown:

$$\langle \mathbf{D}_k * \mathbf{D}_{k+1} \rangle = \langle \mathbf{d}_k * \mathbf{d}_{k+1} \rangle + \langle \delta_k * \delta_k \rangle \tag{7}$$

where $\mathbf{D}_k$ is an error-free displacement and $\boldsymbol{\delta}_k$ is the vector measurement error associated with the kth measured displacement. This equation states that the true step-lag-one autocorrelation value is greater than the measured value by the variance of the measurement errors. For step-lags greater than one, no correction is required. Analogous relations may be obtained for magnitude correlations, valid for long paths (large N) and uncorrelated errors. The displacement magnitude correction is given by

$$R_{DD}(1) = R_{dd}(1) + \frac{1}{N} \sum_{j=1}^{N} \delta_j^2 \tag{8}$$

By expanding the dot product an approximate correction to $\cos\theta$ correlation may be calculated from Eq. 7 for small errors as

$$R_\theta(1) = R_\theta(1) + \langle (\delta/d)^2 \rangle \tag{9}$$

where (δ/d) is the ratio of measurement error to measured one-step cell displacement. We have estimated the measurement error by performing several video "tracking" experiments on unmoving fluorescent beads of about the same size as a neutrophil. We identify the magnitude of the vector measurement error δ, required by Eqs. 7–9 with the average magnitude of the bead displacements. This set of measured displacements is Gaussian and randomly directed, with a magnitude of 0.0960 microns. We have therefore incremented our step-lag one autocorrelation values by 0.0092 and 0.0054 for the displacement and $\cos\theta$, respectively. In the case of error/error or error/displacement correlation, one could find much larger corrections. No results presented here would be changed if the estimated error were several times larger.

The partial autocorrelation function (PAC) and associated t-test were calculated following Bowerman and O'Connell (1987). Measurement error-corrected values of the step-lag-one autocorrelation function were used. Bowerman suggests a t-test significance level of $t \geq 2.0$. For our data, this value would nominally represent about 3 times the SE (Bartlett, 1946). We considered how secure a measure of significance this criteria provides; are non-Markov correlations a frequently produced artifact of our own random data? As a test we randomly extracted continuous 50 step samples (subpaths) of displacements and turn angles from all globally Markov paths. After discarding from the sample those subpaths that proved to be non-Markov (local non-Markov behavior), we randomly concatenated groups of four subpaths to produce pseudo-paths of length 200 steps. In our sample of pseudo-paths (N = 500), no instance of non-Markov correlation was observed in the assembled 200 step pseudo-paths. We also constructed 200 step pseudo-paths by concatenating 50 step non-Markov subpaths. This procedure always produced a series non-Markov in the turn angle or displacement variable. By these measures, the above t-test criterion consistently reports the presence of dominant non-Markov behavior in our data sets or subsets, while rejecting with high probability all purely Markov behaviors. We also take these results to imply that, for the data sets analyzed, the question of stationarity is not of primary significance in the assertion of global non-Markov behavior. We may, however, misjudge a non-Markov path as Markov, because several of the globally Markov paths have small numbers of non-Markov subpaths, e.g., local non-Markov behavior within a globally Markov path.

Partial autocorrelation acts as a filter. Assuming that the experimental step size (time to acquire one image or image-pair) is less than the decay time ($1/\beta$) of the biophysical process, apparent system memory will be reduced to one experimental step-time by elimination of intervening correlations during this step. Any correlation between separated elements of the time series independent of intervening correlations will pass through the

filter. If the experimental step-time is much bigger than $(1/\beta)$, then correlations will not exist even for one step-lag. The importance of the partial autocorrelation technique for identifying system memory has been emphasized by Dunn and Brown (1987).

Numeric representations of the cell perimeter are an attempt to partition cell behaviors such as turning, searching, and extension, according to quantitative shape measures. Such shape measures will, at a minimum, have a low and high order component (Kieler et al., 1989). As a practical consequence, shape vector component values may be quite sensitive to local displacements in the cell. We construct shape vector components from the Fourier and elliptical Fourier decomposition of the cell perimeter difference function. The Fourier decomposition produces one set of harmonic coefficients; the shape vector component Ru that we apply in this study is built from the 5th, 6th, and 8th harmonic (Hartman et al., 1993a). The elliptical Fourier transform produces four sets of harmonic coefficients (Diaz et al., 1989). From these four sets of harmonics coefficients, lengths of semi-axis may be calculated and different shape vectors produced. Shape vector component E2, analogous to Ru, is built from the semi-axis pair at the 4th harmonic.

RESULTS

Characterization of PMN behavior

Fig. 1 demonstrates representative paths of neutrophils moving in the absence of applied stimulation. The centroid of the cell is measured every 4 s. We examined 37 paths from experiments performed on several days. The mean velocity was 17 ± 11 μ/min, and the rms turn angle was 75 ± 53 degrees based on a sampling period of 4 s. The same data, when sampled at 36 s intervals, had a mean velocity of 9.9 ± 6.3 μ/min. Displacements calculated from paths sampled at longer time periods reflect iterations of these smaller displacements and result in the same velocities reported by other investigators (Howard, 1982). Because a PMN is about 10 to 20 μ in diameter, it takes about 90 s for the cell to translocate across its diameter. Thus, on a small time scale, the centroids plotted in Fig. 1 reflect differential subcellular displacements

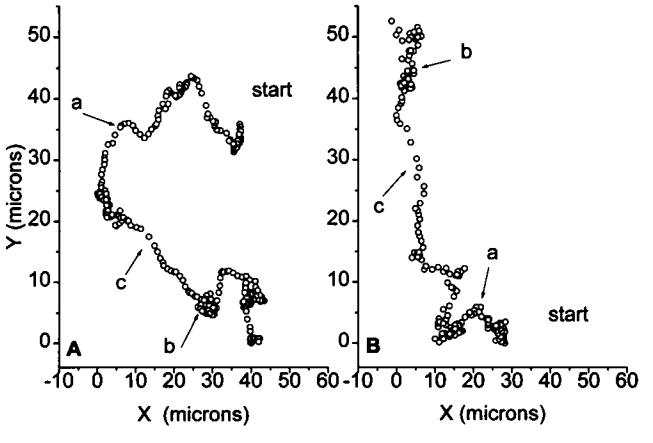

FIGURE 1 Paths of unstimulated neutrophils at 37°C. Coordinate values are expressed in microns and translated along each axis to make the smallest coordinate values equal 0. Labels a, b, and c identify positions along the path of characteristic patterns of large turns, searching, and persistence, respectively. Panel *A* shows a track ($N = 300$) globally Markov in both displacement and turn angle. Panel *B* shows a track ($N = 211$) globally non-Markov in displacement and turn angle. Mean square displacements for these cells are similar.

(shape change). The large mean turn angle and variance reflect the rapid sampling rate relative to the time required for net cell translocation. The PMN centroid is shifting perpendicular to its mean path as the cell produces small lateral undulations in the shape of the PMN edge. Thus, the turn angles at 4 s intervals are relatively large, even during net straight line motion (Fig. 1, region c). In other words, the length and straightness of the path depend upon the scale of the observation.

To determine if the motile behavior observed under our experimental conditions was similar to that seen by previous investigators, mean square displacement ($\langle h^2 \rangle$) for each of the PMN paths was plotted against time for path step ranges of 1–25 and 1–60. For this study, we have excluded all cell paths with values of $\langle h^2 \rangle$ less than 50 μ^2 at 25 steps as not sufficiently "active."

For the plots in the step range 1–25, all 37 paths fit the worm-like-chain relation quite well when standard measures of fit were utilized. Fig. 2 *A–D* present examples typical of this agreement covering an order of magnitude in h^2. We therefore obtain $\langle h^2 \rangle$ vs. t results that are in agreement with previously published results when similar analysis is employed. By this criterion, we conclude that the behavior observed under our experimental conditions is similar to that seen by others and would have been considered to follow the WLC relation.

Non-Markov behavior

Markov correlation of sequential PMN displacements is the simplest outcome consistent with the WLC behavior of PMN just described. We have examined the cell paths by partial autocorrelation analysis (Bowerman and O'Connell, 1987). Using this technique, non-Markov behavior of the displacement or turn angle is judged by performing a t-test at each step of the partial autocorrelation function for the variable. If the function value does not uniformly decay for short step-lags and the correlation is significant by t-test (>2.0), then the path can not be Markov. Fig. 3, *A* and *B* show examples of non-Markov autocorrelation behavior for turn angle ($\cos\theta$) and displacement magnitudes obtained from two PMN tracks. The angle correlation at step-lag 5 (20 s) in Fig. 3 *A* is significant at the 0.01 level. The fact that the partial autocorrelation increases significantly between step one and step five is direct evidence for programmed cell behavior. Fig. 3 *B* shows similar behavior for the displacement magnitude variable. Such correlations were observed between the 2nd and 12th step-lag in 24 of the 37 paths analyzed. The data are summarized in Table 1. Of these 24, we identified 20 paths that showed significant non-Markov correlation in either turn angle (9 cells) or displacement (11 cells), with 4 paths showing significant correlations in both.

Although it is common procedure (Bartlett, 1946) in time series analysis to subset the path and construct an average autocorrelation function, this technique may be misleading. Fig. 4, *A* and *C* are histograms of correlations at step-lag 5 obtained by sub-setting the globally non-Markov paths

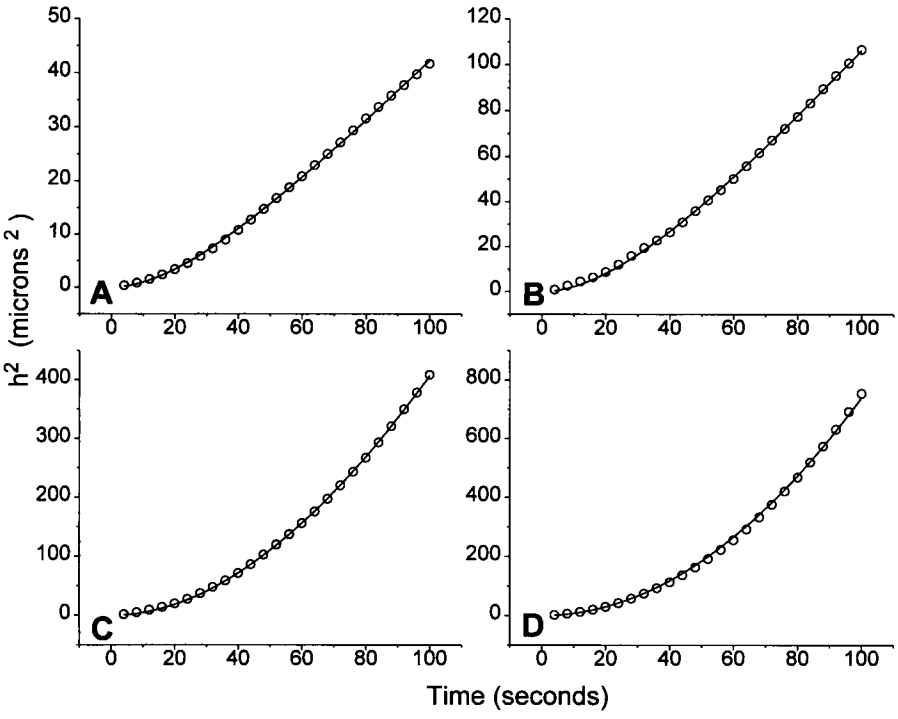

FIGURE 2 Representative experimental mean square displacement vs. time relations derived from cell paths with differing extents and calculated over step displacements from 1 to 25. The data were obtained from neutrophils crawling on albumin-coated glass coverslips at 37°C and imaged at 4 s per step. The solid line is the least-squares fit of the WLC relation (Eq. 1) to the data. Panels *A–D* are ordered by maximum value of h^2 and reflect net cell displacements from 7 to 26 microns in 100 s.

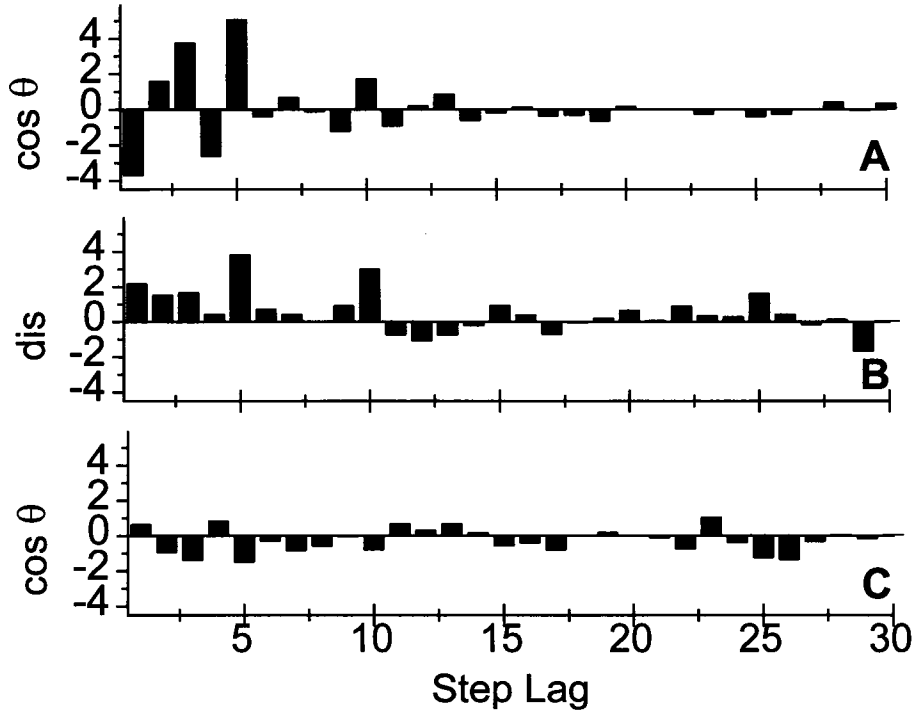

FIGURE 3 Experimental autocorrelations for paths judged non-Markov. The turn angle and displacement are represented by the PAC t-test function. Significant non-Markov correlations require $t > 2$, and the function does not uniformly decay away from the value at step-lag one. Panel *A* shows non-Markov correlations in turn angle. Panel *B* shows non-Markov correlations in displacement. Panel *C* shows correlations after resampling data in panel *A* at every 8th value, giving 32 s/step rather than 4 s/step. By this resampling process, representing data acquisition at a lower frame rate, all correlations even to the 1st step-lag have been eliminated. For all three panels, the 1st data point is the step-lag = 1 value.

represented in Fig. 3. Fig. 4, *B* and *D* are examples of PAC functions derived from 50 step segments within the same data sets, and show the same correlation detected by the global function. Similar bimodality in correlation of each variable was observed in each globally non-Markov path. For example, if the PAC is significant at step-lag 3 for the global function, then the distribution of correlations for step-lag 3 of the sub-paths will be bimodal. A non-Markov correlation

TABLE 1

Non-Markov cos θ	Non-Markov |d|	Non-Markov cos θ and |d|	Markov cos θ and |d|	Total
9	11	4	13	37

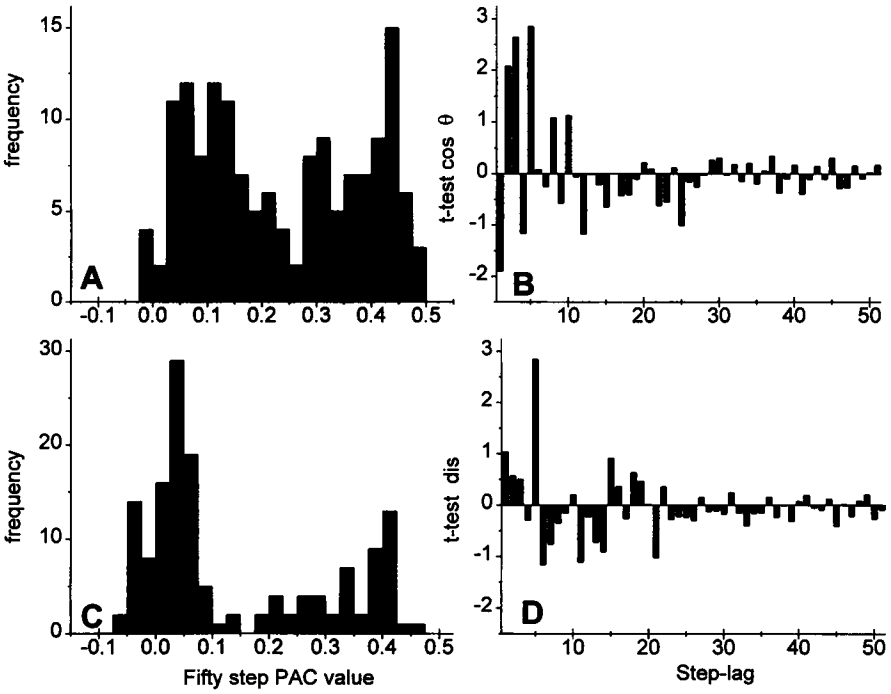

FIGURE 4 Bimodal dispersion of PAC values for subpaths of PMN tracks judged globally non-Markov. Panels *A* and *C* show the histograms of local (50 step) PAC values for the 5th step-lag in turn angle and displacement. In each case, the mode is near 0.05 and 3.5 reflect Markov and non-Markov behavior, respectively. Panels *B* and *D* demonstrate sample 50 step PAC function (t-test values) from the "correlated" peak of the turn angle and displacement bimodal distributions, respectively. The significant correlation at step-lag 5 is clear in both. Data for this figure were extracted from the non-Markov paths shown in Fig. 5. The global non-Markov behavior can be seen to reflect quantitatively the local non-Markov behavior.

in the whole path may occur for two reasons: either the correlations are distributed uniformly throughout the path or they exist in a significant fraction of the sub-paths. The clear bimodality in distribution of subpath correlations in Fig. 4 suggests the non-Markov behavior is nonuniformly distributed. For such data, a correlation function constructed by an average over subpaths does not represent a central tendency of the data and obscures the significant subpopulation of correlated movements detected by the global autocorrelation.

Fig. 3 *C* demonstrates the results of resampling the Fig. 3 *A* turn angle data at 32 s intervals. No significant correlation exists between adjacent values as one would expect from a totally random (Markov-0) process. Obviously, fundamental misunderstanding of cell processes results from undersampling of cellular movement. Thus, we have demonstrated that decreasing the sampling rate from 4 s per sample to 32 s per sample converts programmed movement into apparent random movement.

In contrast to the preceding data, we detected Markov behavior in 13 of 37 paths analyzed. In only four instances did a variable show totally random (Markov-0) behavior. Fig. 5 *A* gives a representative example of Markov-1 autocorrelation in turn angle data. Note that there is significant correlation only for the first step. This figure gives us some sense of the background noise in our experimental system. The autocorrelation background seen at large step-lags is partially attributable to sampling noise and is about 15% of the peak correlation values. This result compares favorably with the value of about 25% reported by Dunn and Brown (1987) in an autocorrelation study of fibroblast movement. Fig. 5 *B* gives an example of a Markov displacement PAC for which decaying but significant correlations at lags greater than one are evident. For globally Markov paths, distributions of correlations in subpaths tend to be centered around a low value at all step-lags greater than one as illustrated by the histogram of step-lag 5 PAC data in Fig. 5 *C*.

In an arithmetic sense, this may not seem interesting because the averaged correlations over 50 step subpaths are always Markov and the $\langle h^2 \rangle$ values are averaged over similar order lengths. However, although stationary time series may be judged by this criterion, the details of neutrophil movement require a different insight. The non-Markov behavior is not uniformly smeared throughout the cell path, but evidenced clearly in a set of subpaths. The fact that a significant number of subpaths can be found in the non-Markov mode of the bimodal histogram makes the global correlations numerically non-Markov. Bimodality as a physical "strategy" of translation may give the PMN an opportunity to move in a straight line and opportunities to change direction.

Evidence for a periodic driving process

Based on the above observations of programmatic neutrophil behavior, we looked for independent evidence of regularities in neutrophil movement. The fundamental unit of neutrophil movement is shape change. Others have seen oscillation in right angle scattering, thought to reflect shape change, within suspensions of neutrophils (Wymann et al., 1990). Likewise, periodic changes in shape of moving neutrophils have been observed (Senda et al., 1975). To detect and quantify such periodicities, we followed the time evolution of neutrophil shape using frequency space shape descriptors that are sensitive to extension and curvature of the cell perimeter (Zahn and Roskies, 1972; Diaz et al., 1990; Hartman et al., 1993a).

The contour of the neutrophil perimeter was represented by a two-dimensional frequency space shape vector (Rv:Ru)

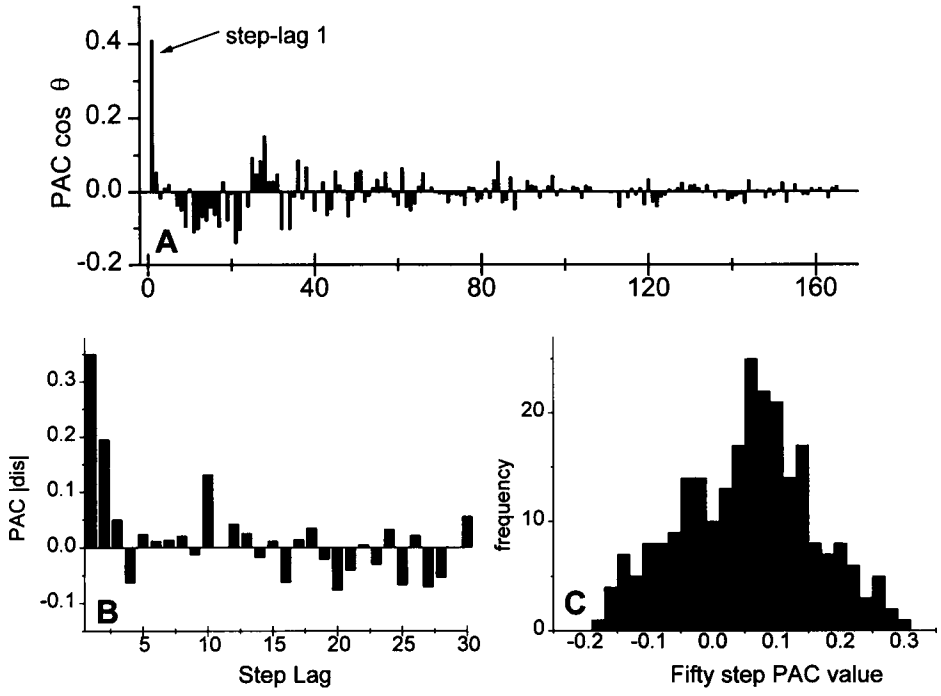

FIGURE 5 PAC for globally Markov paths. Panel *A* shows a Markov 1 path. Panel *B* shows a Markov path with significant correlations extending to several steps. The distribution of local PAC values at all step-lags does not show the strong bimodality seen in globally non-Markov paths. Panel C shows a representative distribution of step-lag 5 PAC values for all 50 step subpaths in a globally Markov path. In this case, there are few subpaths displaying significant correlations.

(Hartman et al., 1993a), or E1:E2 using elliptical transforms at each position along the path of movement, as described in Materials and Methods. The shape vector components Ru and E2 were designed to be particularly sensitive to small focal variations in neutrophil shape. This was accomplished by utilizing spatial frequency components of the Fourier or elliptical Fourier transform of the PMN edge difference function that are relevant to features of interest. Cyclic variation in a plot of Ru or E2 as a function of time would indicate cyclic variations in cell contour. The technique of sequential Fourier transforms, first in the spatial domain of the cell perimeter and second in the time domain of cell movement, was pioneered for analysis of cell motility by Partin et al. (1989). Identification of prominent recurring cell shapes may be accomplished by examination of the frequency spectrum of the plot of Ru or E2 versus time.

Within the time scale defined by the non-Markov correlations of displacement and turn angle, we observed a

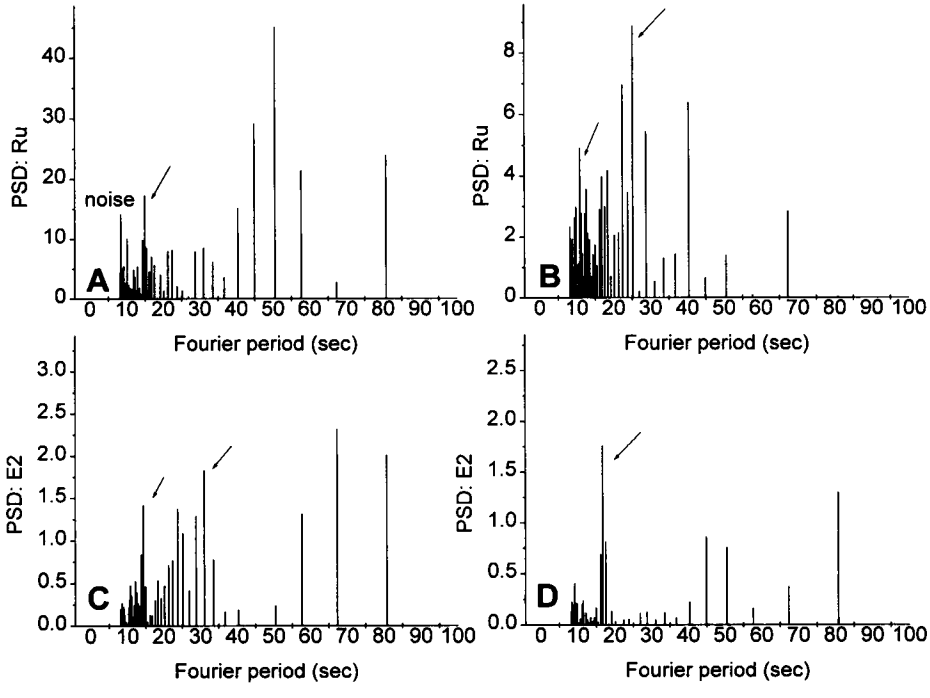

FIGURE 6 Power spectrum of shape descriptor components used to follow shape changes in moving PMN. Arrows (→) mark Fourier components of shape change that may be related to non-Markov correlations in movement variables. Panels *A* and *B* display the high frequency "time" spectrum for the spatial Fourier transform-derived shape vector component Ru. Panels *C* and *D* display the same spectrum for the elliptical Fourier transform-based component E2. In panels *A* and *D*, one high frequency peak of 12–17 s is evident; the high frequency noise peak has been labeled in panel *A*. Panels *B* and *C* show two high frequency peaks with the lower frequency peak between 20 and 30 s. Note that the abscissa does not start at zero frequency but at short times. Components near these frequencies have been detected in several motion parameters in addition to perimeter contour.

periodic component to neutrophil shape change. Fig. 6 *A–D* demonstrate cyclic variation in neutrophil shape measured by Ru or E2, in four cells with characteristic WLC paths. The power spectral density of each 50 step segment demonstrates the presence of important components with periods of approximately 15 or 25 s, or both. Although these components may be identified by a global analysis of some non-Markov paths, analysis that focuses on non-Markov subpaths provides more convincing results. Dembo (Dembo, 1989), in a theoretical treatment of fountain streaming in *Amoeba proteus* found 12 s as the fundamental decay time for the cytoskeleton elements permitting the flow of cytoplasm. The apparent higher frequency component in Fig. 6, *A* and *B* is not well separated from the high frequency noise spectrum. Although all of the apparent high frequency components may suffer from being close to the Nyquist limit (t = 8 s), both upper and lower frequency peaks may also be observed for E2 in Fig. 6, *C* and *D*. The power spectral peak that sometimes appears in time range 50–80 s may reflect locally a systematic change in PMN shape associated with major pseudopod extension. This measurement is consistent with a theoretical calculation of 70 s periodicity for "slow" lamellipod extension and retraction in leukocytes that was based upon local changes in surface tension of the plasma membrane (Alt, 1990).

We are persuaded that both an upper and lower frequency peak exist in the time frame 10–30 s. In Fig. 7 we have plotted the power spectral density function for the vector displacement autocorrelation. This autocorrelation function, defined by Eq. 5 and corrected by Eq. 7, is averaged over 32 steptimes of seven cell tracks displaying global non-Markov PAC behavior. The frequency components near 10 and 20 s are unambiguous. The correlations in PMN movement are much more easily seen using vector variables than by separately analyzing turn angles and displacements, although strong evidence of the nonvector correlations may be demonstrated (Fig. 3). Taken as a whole, the autocorrelation and shape change data give clear evidence for programmatic, and in fact cyclical, change in shape in motile neutrophils.

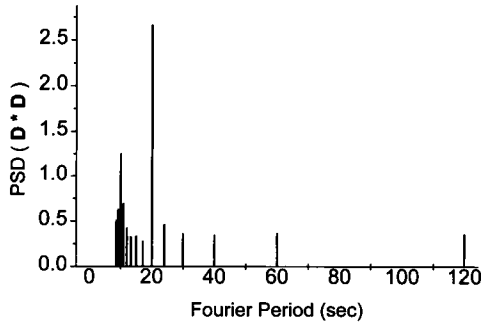

FIGURE 7 Power spectrum of vector displacement autocorrelation function ($D \cdot D$). We obtain this spectrum by calculating and averaging vector correlations over 32 step subpaths and performing the Fourier transform on the averaged value. The data set consists of 7 PMN tracks judged globally non-Markov by correlation in displacement magnitude.

DISCUSSION

The search for the fundamental motor of single cells capable of directed motion has attracted many investigators and resulted in many hypotheses (Stossel, 1990, 1993). In general, the problem has been approached from two directions: 1) the study of gross cell motion by means of tracking experiments and 2) investigation of the biochemistry of cytoskeletal and contractile proteins such as actin and myosin. The smallest unit of cell motility is shape change. It is at this level that studies of motion and biochemistry converge (Stossel, 1993). At some point, changes in shape must be explainable by local differences in force that are, in turn, the result of local biochemical processes. Iterations of shape change then result in net cell translocation. This scenario inherently implies a repetitive or cyclic process. Indeed, early observers (Senda et al., 1975) and anyone who has watched time-lapse videos of moving neutrophils note rhythmic undulations in the cell as it traverses a surface.

One way to derive information about the fundamental process driving cell motility is to fit an experimentally determined motion variable to a well described theoretical model. A critical point in this approach is that the macroscopically measured variable is sampled at a rate fast enough to detect the underlying physical process. In the case of the neutrophil, the sampling rate should be faster than the time required for shape change, if cell velocity is to be explained by iterations of shape change. The worm-like-chain relation for mean-squared displacement (WLC; Eq. 1) has been used by several investigators to describe motion of single motile cells (Gail and Boone, 1970; Tranquillo et al., 1988; Bültmann and Gruler, 1983; Stokes et al., 1991; Tranquillo and Lauffenburger, 1987; Gruler, 1993). The rationale for its use is sound, namely, it describes a locally persistent and globally random process. As we and others have found, neutrophil displacements appear to follow this equation very well. A significant technical problem arises when one tries to determine whether any experimental data are in agreement with the WLC expression for $\langle h^2 \rangle$ vs. t because displacements for long times are necessarily correlated with displacements for short times. This makes standard curve-fitting techniques inaccurate for all but the shortest displacements.

We had observed periods of evident nonrandom motion in spontaneously migrating PMN whose position was sampled at short time intervals. This led us to question previous assertions that the fundamental driving process of PMN motility is random. To address this question, we examined PMN motile behavior using partial autocorrelation, Fourier analysis of shape change, and conventional $\langle h^2 \rangle$ vs. t plots. Partial autocorrelation analysis was applied to turn angle and displacement data because it provides a reasonable test of correlation between separated members of a time series. This test eliminates long-range correlations that may arise because of chains of very short range correlation (Bowerman and O'Connell, 1987; Dunn and Brown, 1987). The unexpected result is that apparent WLC path behavior is associated with

non-Markov, programmatic correlations on a time scale consistent with observed periodic fluctuations in cell shape.

The apparent agreement between the WLC (Eq. 1) and cell tracking data has led a number of authors to propose the Langevin equation (Eq. 3) as a model governing cell behavior. In particular, this assertion has been made for neutrophils (Parkhurst and Saltzman, 1992), endothelial cells (Stokes et al., 1991), and fibroblasts (Dunn and Zicha, 1993). The biological implications are profound. Only by assuming a zero mean, velocity-independent, random driving impetus (Doob, 1942) may Eq. (1) be derived from Eq. (3). The cell motor must be conceived as utterly disconnected from its own action and the cell environment. Once these constraints on the cell motor are assumed, the Markov property of cell movement parameters is a necessary mathematical consequence. Our data demonstrating non-Markov correlations in cell displacements and turn angles suggest that the "random impetus" model is not adequate to characterize motile behavior of all PMN. In fact, only 13 of 37 cell tracks studied were judged to display Markov behavior in both turn angles and displacements, and no cell had Markov-0 (random) behavior in both parameters.

Boyarski and Nobel (1977) reported a successful description of neutrophil movement according to a Markov model. The analysis measured diffusion out of a current state of motion defined by the next direction (quadrant), or no motion. An exponential decay with time out of the current state (Markov) is expected. The experimental conditions under which the neutrophil movement was quantified suggest that a nonrandom component to cell behavior could have been obscured. In particular, the frame rate was low (8 s/frame), all displacements less than half a cell diameter were counted as no motion, the cell density was high, and the total observation time was short (80 s). The authors indicate that they are quite aware of the influence these factors might have. Despite these constraints, the distribution data presented in the paper do not seem to us to support simple exponential decay away from the current direction of cell movement. The disagreement is particularly evident for the "no movement" state. Interestingly, Bültmann and Gruler (1983) suggests the Boyarski and Noble data supports a "programmatic" model of movement. We purposely looked at low cell concentration, with rapid sampling and relatively long observation times, to avoid confusing effects of cell-cell interaction.

Bültmann and Gruler (1983) observed that the distribution of turn angles for moving human granulocytes does not randomize as would be expected based on a Markov process. Instead of exponential time decay toward a uniform distribution, he finds a step-function behavior with a subsequent preferred turn angle of about fifty degrees. He assigned the nonexponential decay of order to a cell program of 32 s duration. When we studied neutrophil paths that were highly correlated (Fig. 3 *A*), reducing the sampling rate from 4 to 32 s per point was sufficient to randomize this otherwise correlated function (Fig. 3 *C*). This is in good agreement with the observations of Bültman. The question is: what process is randomized in 32 s?

The authors admit to little guidance in this matter from current theories of cell motility. The difficulties are twofold. Some current theories address extension of a single lamellipod based on local opportunistic expansion (Zhu and Skalak, 1988; Oster, 1984; Odell, 1984) at the site of a plasma membrane "weakness" but do not address processes that can be executed repetitively and can therefore lead to net cell motion. The latter, repetitive aspect could easily become randomized. Moreover, plasma membrane weakness theories require a solid backstop of cortical gel at the very point of expansion. We have observed quite the opposite in suspended PMN (Coates et al., 1992) where the entire actin cortex dissolves at the point of pseudopod extension.

The model of *Amoeba proteus* devised by Dembo provides another mechanism of lamellipod extention but is uniaxial. He suggests that the organization of major cytoskeletal elements is a consequence of the global flow field and reaction kinetics (Dembo, 1989). This is no problem for a one-dimensional organism. However, it seems likely to us that several quasi-simultaneous axes of flow are required if a fountain flow model is to be constructed for the neutrophil. Alt (1990) alludes to the existence of similar modes in circular, unpolarized cells and Dembo et al. (1986) observes "rending modes" in contracting gels. It is possible that natural internal boundaries for such flows exist in polarized cells such as the PMN.

The patterns in neutrophil movement we have observed are almost certainly not measures of whole cell translocation. At an average cell speed of 0.17 μ/s and a length of 15 μ, the cell needs 90 s to move free of its previous position. The unstimulated neutrophil does not move in leaps as a unit. Rather, the movement is better ascribed to local multidirectional cytoplasmic flows individually producing local extensions and contractions at the perimeter of the cell. Spatial and temporal organization of these flows produces the measured local displacement of the entire cell. This behavior has been qualitatively described long ago (Senda et al., 1975). Rhythmic undulations in cytoplasmic flow and neutrophil shape have even led to the suggestion of cytoplasmic waves powering cell motion (Durham, 1974; Stossel, 1993). There are clearly perceptible undulations in neutrophil shape as the cells seem to glide along their paths. Our time series studies of the shape vector component Ru and E2 (Hartman et al., 1993a) detect these undulations and identify prominent frequency components at about 10 and 20 s periods. This timing is comparable with the period described by Senda et al. (1975) in his visual studies of crawling neutrophils. It is also similar to the 10 s oscillations in light scattering observed by Wymann in suspensions of PMN (Wymann et al., 1990). Light scattering is closely linked to actin polymerization, a process thought to be critical in neutrophil shape change and motion (Coates et al., 1992; Omann and Painter, 1985; Wymann et al., 1990; Omann et al., 1989). Notably, the magnitude of these oscillations in scattering decays over 40 s,

approximately the same time required for randomization of the correlated movement in our tracking studies. It is premature to claim that the decaying oscillations in actin content detected by light scattering and the high frequency shape changes we see in our tracking experiments are the same; however, this hypothesis would provide one attractive candidate process that could explain our experimental data.

This paper provides direct experimental evidence that apparent fit of neutrophil motion data to the worm-like-chain equation does not imply random behavior or, more importantly, a random fundamental driving force. Furthermore, we present direct measurements of cyclic shape change in moving neutrophils, demonstrating one type of correlated, time scale-dependent behavior that may characterize the neutrophil motor. Although we can not specifically identify the process that drives neutrophil motion, our data give clear evidence for programmatic and, in fact, cyclical change in shape in neutrophils whose sequential displacements are non-Markov. If the fundamental cyclical driving force were directly translated into movement, then the neutrophil displacement magnitudes would be cyclic. Would our proposed periodic cell motor be consistent with our observed non-Markov cell displacements? In general, a sinusoidal function of finite duration will have a sinusoidal, damped autocorrelation function. The data we presented using autocorrelation of the amplitude of displacement and turn angle are insufficient to demonstrate this. However, any time series created by differencing successive elements of a cyclic process will display a non-Markov partial autocorrelation function, as discussed in Bowerman and O'Connell (1987) and demonstrated in the neutrophil motility data in Fig. 3. The biologic property of the cell that transforms the fundamental programmatic impetus into net displacement remains to be identified. Nonetheless, our data support a cyclical or deterministic component to the overall mechanism of neutrophil motility.

This work was supported by National Institutes of Health grant AI23547 to T. D. Coates.

REFERENCES

Allen, R. B., and P. C. Wilkinson. 1978. Avisual analysis of chemotactic and chemokinetic locomotion of human neutrophil leukocytes. *Exp. Cell Res.* 111:191–203.

Alt, W. 1980. Biased random walk models for chemotaxis and related diffusion approximations. *J. Math. Biology.* 9:148–165.

Alt, W. 1990. Mathematical models and analysing methods for the lamellipodial activity of leukocytes. *In* Biomechanics of Active Movement and Deformation: NATO ASI Series, Vol. H42. N. Akkas, editor. Springer-Verlag, Berlin. 403–422.

Baggiolini, M., and P. Kernen. 1992. Neutrophil activation: control of shape change, exocytosis, and respiratory burst. *NIPS.* 7:215–219.

Bartlett, M. S. 1946. On the theoretical specification of sampling properties of autocorrelated time series. *J. R. Stat. Soc.* B8:27–33.

Bowerman, B. L., and R. T. O'Connell. 1987. Nonseasonal Box-Jenkins models and their tentative identification. *In* Time Series Forecasting. Duxbury Press, Boston, MA. 31–46.

Boyarski, A., and P. B. Nobel. 1977. A Markov chain characterization of human neutrophil locomotion under neutral and chemotactic conditions. *Can. J. Physiol. Pharmacol.* 55:1–6.

Boyum, A. 1984. Separation of lymphocytes, granulocytes, and monocytes from human blood using iodinated density gradient media. *In* Methods in Enzymology: Immunochemical Techniques. Part G. G. di Sabato, J. J. Langone, and H. van Vunakis, editors. Academic Press, New York. 88–102.

Bültmann, B. D., and H. Gruler. 1983. Analysis of the directed and non-directed movement of human granulocytes: influence of temperature and ECHO 9 virus on N-formylmethionylleucylphenylalanine-induced chemokinesis and chemotaxis. *J. Cell Biol.* 96:1708–1716.

Cassimeris, L., and S. H. Zigmond. 1990. Chemoattractant stimulation of polymorphonuclear leucocyte locomotion. *Cell Biol.* 1:125–134.

Coates, T. D., M. Torres, J. Harman, and V. Williams. 1987. Localization of chlorotetracycline fluorescence in human polymorphonuclear neutrophils. *Blood.* 69:1146–1152.

Coates, T. D., R. G. Watts, R. Hartman, and T. H. Howard. 1992. Relationship of F-actin distribution to the development of polar shape in human polymorphonuclear neutrophils. *J. Cell Biol.* 117:765–774.

Dembo, M. 1989. Mechanics and control of the cytoskeleton in *Amoeba proteus*. *Biophys. J.* 55:1053–1080.

Dembo, M., M. Maltrud, and F. Harlow. 1986. Numerical studies of unreactive contractile networks. *Biophys. J.* 50:123–137.

Diaz, G., D. Quacci, and C. Dell'Orbo. 1990. Recognition of cell surface modulation by elliptic Fourier analysis. *Comput. Methods Program Biomed.* 31:57–62.

Diaz, G., A. Zuccarelli, I. Pelligra, and A. Ghiani. 1989. Elliptic fourier analysis of cell and nuclear shapes. *Comput. Biomed. Res.* 22:405–414.

Dickinson, R. B., and R. T. Tranquillo. 1993. Optimal estimation of cell movement indices from the statistical analysis of cell tracking data. *AIChE J.* 39:1195–2010.

Doob, J. L. 1942. The Brownian movement and stochastic equations. *Ann. Math.* 43:351–369.

Dunn, G. A., and A. F. Brown. 1987. A unified approach to analysing cell motility. *J. Cell Sci.* 8:81–102.

Dunn, G. A., and D. Zicha. 1993. Long-term chemotaxis of neutrophils in stable gradients: preliminary evidence of periodic behavior. *Blood Cells.* 19:25–41.

Durham, A. C. H. 1974. A unified theory of the control of actin and myosin in nonmuscle movements. *Cell.* 2:123–136.

Dvorak, J. A., and W. F. Stotler. 1971. A Controlled-environment culture system for high resolution light microscopy. *Exp. Cell. Res.* 68:144.

Einstein, A. 1905. Uber Die von der molekularkinetischen theory der warme geforderte bewegung von in ruhenden flussigkeiten suspendierten teilchen. *Ann. Phys.* 7:549–560.

Gail, M. H., and C. W. Boone. 1970. The locomotion of mouse fibroblasts in tissue culture. *Biophys. J.* 10:980–993.

Gruler, H. 1993. Directed cell movement: a biophysical analysis. *Blood Cells.* 19:91–113.

Gruler, H., and B. D. Bültmann. 1984. Analysis of cell movement. *Blood Cells.* 10:61–77.

Hartman, R. S., K. Lau, W. Chou, and T. D. Coates. 1993a. Development of a shape vector that identifies critical forms assumed by human polymorphonuclear neutrophils during chemotaxis. *Cytometry.* 14: 832–839.

Hartman, R. S., D. Yi, and T. D. Coates. 1993b. Analysis of multi-parameter video measurements of human neutrophil movement and its relation to cell shape and cytosolic calcium. *Comput. Methods Program Biomed.* 39:195–201.

Harvey, A. C. 1993. Time Series Models. MIT Press, Cambridge, MA. 42 pp.

Howard, T. H. 1982. Quantification of the locomotive behavior of polymorphonuclear leukocytes in clot preparations. *Blood.* 59:946–951.

Howard, T. H., D. Wang, and R. L. Berkow. 1990. Lipolysaccharide modulates chemotactic peptide induced actin polymerization in neutrophils. *J. Leukocyte Biol.* 47:13–24.

Jaconi, M. E., J. M. Theler, W. Schlegel, R. D. Appel, S. D. Wright, and P. D. Lew. 1991. Multiple elevations of cytosolic-free Ca^{2+} in human neutrophils: initiation by adherence receptors of the integrin family. *J. Cell Biol.* 112:1249–1257.

Jaconi, M. M., R. W. Rivest, W. Schlege, C. B. Wolheim, D. Pittet, and P. D. Lew. 1988. Spontaneous and chemoattractant-induced oscillations of cytosolic free calcium in single adherent human neutrophils. *J Biol. Chem.* 263:10557–10560.

Kieler, J., W. Skubis, P. S. Grzesik, J. Wisniewski, and A. Dziedzic-Goclawska. 1989. Spreading of cells on various substrates evaluated by fourier analysis of shape. *Histochemistry.* 92:141–148.

Kleinrock, L. 1975. Queuing Systems, Vol. 1: Theory. John Wiley & Sons, New York.

Landau, L., and E. Lifshitz. 1958. *Stat. Phys. A.* 478–482.

MacFarlane, G. D., M. C. Herzberg, and R. D. Nelson. 1987. Analysis of polarization and orientation of human polymorphonuclear leukocytes by computer-interfaced video microscopy. *J. Leukocyte Biol.* 41:307–317.

Nafe, R., S. Roth, and P. Rathert. 1991. Fourier analysis as a planimetric procedure application to malignant and normal urothelial cells with reactive changes. *Exp. Pathol.* 43:155–167.

Needham, D., and R. M. Hochmuth. 1992. A sensitive measure of surface stress in the resting neutrophil. *Biophys. J.* 61:1664–1670.

Nossal, R., and S. Zigmond. 1976. Chemotropism indices for polymorphonuclear leukocytes. *Biophys. J.* 16:1171–1182.

Odell, G. M. 1984. A mathematically modelled cytogel cortex exhibits periodic calcium modulated contraction cycles seen in *Phys. J. Embryol. Exp. Morph.* 83s:261–287.

Omann, G. M., M. M. Porasik, and L. A. Sklar. 1989. Oscillating actin polymerization/depolymerization responses in human polymorphonuclear leukocytes. *J. Biol. Chem.* 264:16355–16358.

Omann, G. M., and R. G. Painter. 1985. Relationship of actin polymerization and depolymerization to light scattering in human neutrophils: dependence on receptor occupancy and intracellular Ca^{2+}. *J. Cell Biol.* 101: 1161–1166.

Oster, G. F. 1984. On the crawling of cells. *J. Embryol. Exp. Morph.* 83s: 329–364.

Parkhurst, M. R., and W. M. Saltzman. 1992. Quantification of human neutrophil motility in three-dimensional collagen gels. Effect of collagen concentration. *Biophys. J.* 61:306–315.

Partin, A. W., J. S. Schoeniger, and J. L. Mohler. 1989. Fourier analysis of cell motility: correlation of motility with metastatic potential. *Proc. Natl. Acad. Sci. USA.* 86:1254–1258.

Quitt, M., M. Torres, W. McGuire, L. Beyer, and T. D. Coates. 1990. Neutrophil chemotactic heterogeneity to *N*-formyl-methionyl-leucyl-phenylalanine detected by the under-agarose assay. *J. Lab. Clin. Med.* 115:159–164.

Rabiner, L. R., and B. Gold. 1975. Theory and application of digital signal processing. Prentice Hall, Englewood Cliffs, NJ. 401.

Senda, N., H. Tamura, N. Shibata, J. Yoshitake, K. Kondo, and K. Tanaka. 1975. The mechanisn of the movement of leukocytes. *Exp. Cell Res.* 91:393–407.

Stokes, C. L., D. A. Lauffenburger, and S. Williams. 1991. Migration of individual microvessel endothelial cells: stochastic model and parameter measurement. *J. Cell Sci.* 99:419–430.

Stossel, T. P. 1990. How cells crawl. *Am. Scientist.* 78:408–423.

Stossel, T. P. 1993. On the crawling of animal cells. *Science.* 260:1086–1094.

Tranquillo, R. T., and D. A. Lauffenburger. 1987. Stochastic model of leukocyte chemosensory movement. *J. Math. Biol.* 25:229–262.

Tranquillo, R. T., D. A. Lauffenburger, and S. H. Zigmond. 1988. A stochastic model for leukocyte random motility and chemotaxis based on receptor binding fluctuations. *J. Cell Biol.* 106:303–309.

Uhlenbeck, G. E., and L. S. Ornstein. 1930. On the theory of the Brownian motion. *Phys. Rev.* 36:823–841.

Wymann, M. P., P. Kernen, T. Bengtsson, T. Andersson, M. Baggiolini, and D. A. Deranleau. 1990. Corresponding oscillations in neutrophil shape and filamentous actin content. *J. Biol. Chem.* 265:619–622.

Zahn, C. T., and R. Z. Roskies. 1972. Fourier descriptors for plane closed curves. *IEEE Trans. Comput.* C-21:269–281.

Zhu, C., and R. Skalak. 1988. A continuum model of protrusion of pseudopod in leukocytes. *Biophys. J.* 54:1115–1137.